International Journal of Adhesion and Adhesives 85 (2018) 308–314

Contents lists available at ScienceDirect

International Journal of Adhesion and Adhesives

journal homepage: www.elsevier.com/locate/ijadhadh

Thermal and mechanical properties of natural fibrous nanoclay reinforced epoxy asphalt adhesives

Yifan Sun[a], Ya Liu[a], Yongjia Jiang[a], Ke Xu[a], Zhonghua Xi[b], Hongfeng Xie[a,*]

[a] Key Laboratory of High Performance Polymer Materials and Technology of MOE, School of Chemistry and Chemical Engineering, Nanjing University, Nanjing 210023, China

[b] Experimental Chemistry Teaching Center, School of Chemistry and Chemical Engineering, Nanjing University, Nanjing 210023, China

ARTICLE INFO

Keywords:
Epoxides
Nanofillers
Steels
Lap-shear
Scanning electron microscopy
Mechanical properties of adhesives

ABSTRACT

Epoxy asphalt adhesive (EAA) has been widely used as strong waterproof-bonding layers for the orthotropic steel bridge decks in China. This research employs attapulgite (ATT), one kind of natural fibrous nanoclays, as the nanofiller to reinforce EAA. The crystalline structure, rheological property, thermal stability, mechanical properties and morphology of EAA/ATT composites were investigated by X-ray diffraction (XRD), Brookfield rotational viscometer, thermogravimetric analyzer (TGA), universal test machine and scanning electron microscopy (SEM). Results showed the existence of ATT did not change the noncrystalline structure of the EAA. ATT had a significant decrement effect on the rotational viscosity of EAA. Moreover, the viscosity of EAA/ATT composites decreased with the increasing content of ATT at a specific cure time. The addition of ATT improved thermal stability of the neat EAA. In addition, the incorporation of ATT increased the tensile and adhesive properties of the neat EAA. The tensile strength, toughness, Young's modulus and adhesive strength of EAA/ATT composites increased with the increase of ATT loadings.

1. Introduction

Epoxy asphalt (EA) is a two-phase polymer matrix composite formed by dispersing asphalt in the continuous epoxy phase [1,2]. Three main components of EA are epoxy monomer, asphalt and hardener. Irreversible cure reaction between epoxy monomer and hardener gives three-dimensional crosslinking networks around asphalt particles. This thermosetting epoxy modification step enables the transformation of the thermoplastic asphalt into the thermosetting elastomer with the enhancement of thermal stability, strength and durability [3,4]. Due to these characteristics, EA has been widely used as binders for concretes and adhesives (bond coats) for steel bridge decks. Its outstanding resistance to shoving, rutting and cracking allows its application on numerous orthotropic steel decks for long-span bridges all over the world, especially in China [5]. A typical EA overlay for a steel deck is composed of two layer of epoxy asphalt concretes (EAC) (approximately 25 mm) and two layers of epoxy asphalt adhesive (EAA) sprayed onto the steel deck and the underlying EAC layer, respectively. EAA serves as a strong waterproof bonding layer between the steel deck and the EAC layer to withstand the traffic loads monolithically [6]. A failure of bonding layer between the EAC layer and the steel deck may lead to distresses such as debonding, shoving and slippage, which shortens the durability of the overlay system [7]. Therefore, with its high strength and good flexibility, EAA is highly needed to adapt the vibration of the steel bridge deck.

Attapulgite (ATT) is a typical magnesium aluminum silicate with a 2:1 phyllosilicate structure and with the chemical formula of $Si_8O_{20}Mg_5(Al)(OH)_2(H_2O)_4{\cdot}4H_2O$ [8]. The structural unit of ATT is a single fibrillar crystal with the diameter of 20–70 nm and the length of 500–2000 nm. Recently, ATT has attracted tremendous attention as nanofillers for the reinforcement of polymer matrix, because of its unique structure as well as natural fibrous characteristics [9]. However, little work has been published with regard to the reinforcement effect of ATT on epoxy resin and polymer-modified asphalt. Lu et al. [10] proved that the addition of ATT significantly improves storage modulus and dimensional stability of epoxy. Xue et al. [11] compared the influence of pristine and silylated ATT on the properties of rubbery and glassy epoxy matrices. It was found that compared to the pristine ATT-modified epoxies, the silylated ATT-modified epoxies have the improvement of mechanical properties which may stem from the better dispersion of silylated ATT in the rubbery epoxies at low loading levels. However, both pristine and silylated ATT have negligible effects on the tensile properties of glassy epoxy matrices. Zhao et al. [12] investigated the influence of ATT on the phase separation and mechanical properties of

* Corresponding author.
E-mail address: hfxie@nju.edu.cn (H. Xie).

https://doi.org/10.1016/j.ijadhadh.2018.07.005
Accepted 22 June 2018

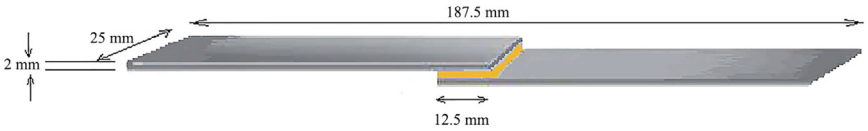

Fig. 1. Joint geometry for the single-lap shear test.

epoxy/poly(ether sulfone) (PES) blends. The final phase-separated morphology of the blends has been changed significantly with the addition of a small amount of ATT. Additionally, the inclusion of ATT improves the modulus of the blends. In order to improve the dispersion stability of ATT in the epoxy matrix, acrylic resin (AC) was used to modify ATT. The introduction of AC-ATT remarkably increases the storage modulus, impact strength, Young's modulus and tensile strength of the neat epoxy [13]. Zhang et al. [14] reported that the addition of ATT improves the compatibility and storage stability of styrene–butadiene rubber (SBR)-modified asphalt.

In our previous study, the influence of ATT on the thermal, mechanical properties, and low-temperature performance of epoxy asphalt binders and their concretes was studied [15]. The incorporation of ATT increases the thermal stability and mechanical properties, especially the toughness of epoxy asphalt binders. In addition, the low-temperature flexibility of the epoxy asphalt concretes is improved with the incorporation of ATT. The aim of present paper is to investigate the effect of ATT on the structure, rheological, thermal and mechanical properties of the EAA used for steel bridge decks. To achieve this goal, ATT reinforced EAA was prepared through the incorporation of ATT into the mixture of hardener and asphalt. The crystalline structure, rheological properties, thermal stability and mechanical properties of EAA/ATT composites were investigated by different characterization techniques. In the meantime, the dispersion of ATT in the EAA matrix was observed with the aid of scanning electron microscopy (SEM).

2. Materials and methods

2.1. Materials

Base asphalt (40/60 penetration grade) was obtained from China Offshore asphalt (Taizhou) Co., Ltd. (Taizhou, China). The epoxy equivalent weight (EEW) of diglycidyl ether of bisphenol A (DGEBA) epoxy monomer is 196 g/eq, supplied by Wuxi Resin Factory (Wuxi, China). The carboxylic acid-based hardener (NDA450B) was prepared in our laboratory. The neat ATT was obtained from Jiangsu Golden Stone Attapulgite R&D Co., Ltd (Nanjing, China).

2.2. Preparation of the EAA/ATT composites

Base asphalt, NDA450B and certain amount of ATT were mixed at 120 °C for 10 min using a FLUKO FM300 high-shear emulsifier (Shanghai, China). Then DGEBA epoxy monomer was added into the mixture of asphalt, hardener and ATT with a weight ratio of 1:4.50. After 5-min high-speed mechanical agitation, the mixture was poured into Teflon molds and cured at 120 °C for 4 h. The loadings of ATT in the EAA composites were 1, 3 and 5 wt%, respectively.

2.3. Characterizations

The crystalline structures of the neat ATT, the neat EAA and EAA/ATT composites were determined by X-ray diffraction (XRD). The XRD patterns were obtained on a Shimadzu XRD-6000 X-ray diffractometer (Japan) with the crystal monochromated Cu K_α radiation at a scanning rate of 5°/min between $2° < 2\theta < 40°$.

The rheological properties of the neat EAA and EAA/ATT composites were measured on a Brookfield rotational viscometer (Model NDJ-1C, Shanghai Changji Instrument Co., Ltd., China). Referring to ASTM D4402, the rotational viscosity was measured at 120 °C with the spindle 28.

Thermal stability of EAA/ATT composites was evaluated by thermogravimetric analyzer (TGA, Mettler Toledo STAR^e System TGA/DSC 1, UK) under a nitrogen atmosphere (40 mL/min). A sample of approximately 10 mg was heated from 50 °C to 600 °C at a heating rate of 20 °C/min.

Tensile properties of EAA/ATT composites were tested on an Instron 4466 universal testing machine (USA), equipped with a 10 kN load cell. The dog-bone specimens for tensile tests were cut by the dumbbell cutter with dimensions of 56 mm × 5 mm × 2 mm. Tensile tests were performed at room temperature with a crosshead speed of 500 mm/min according to ASTM D638. Five experiments were tested for each adhesive.

Adhesive properties of EAA/ATT composites were determined by the single-lap shear test according to ASTM D1002. The uncured mixtures of EAA/ATT composites were first applied to the end of two stainless steel plates (100 mm × 25 mm × 2 mm). Subsequently, two plates overlapped to one another at the length of 12.5 mm with sandwiching the composites and followed by curing reaction (Fig. 1). After curing, the cooled jointed metals are pulled apart using a universal testing machine (Instron 4466, USA) in tension. The lap shear test was carried out on these plates at room temperature at a strain rate of 50 mm/min. Five replicates for the single-lap shear tests were measured for each experiment. Adhesive strengths reported in units of shear stress were calculated as follows:

$$\text{Adhesive strength} = \text{Failure load}/\text{Adhesive lap area} \quad (1)$$

SEM (Hitachi S-4800, Japan) was used to characterize the morphology of the neat ATT and EAA/ATT composites (fractured in liquid nitrogen). SEM samples were coated with gold before imaging.

3. Results and discussion

3.1. Crystalline structure

Fig. 2 shows X-ray diffraction patterns of the neat ATT and EAA/ATT composites. The XRD peaks of ATT appear at the same angular positions as those observed by other researchers [16]. Since calcite and quarts are common carbonate impurities in neat ATT samples, it is not

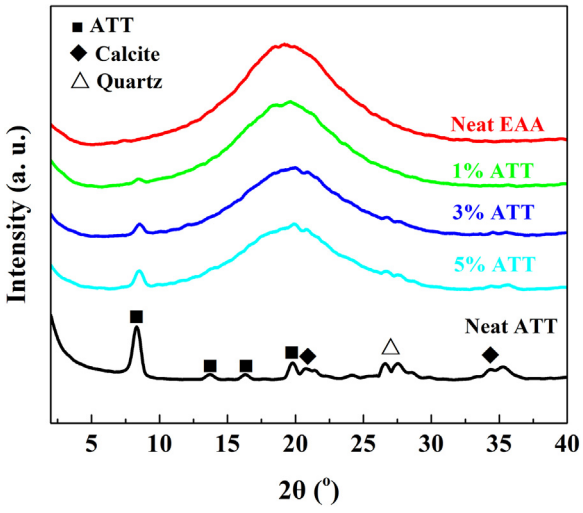

Fig. 2. XRD patterns of the neat ATT and EAA/ATT composites.

surprised to see their characteristic peaks in the XRD. The neat ATT has a d_{110} diffraction peak at 8.4° (2θ) correlated with 1.04 nm interplanar space according to the Bragg equation. Such value is consistent with the reported distance between unit layers in a single crystal [16]. Unit layers cannot further be separated by other polymer matrices so that this characteristic peak would not shift. Therefore we use this peak to identify the loading efficiency of ATT in the composites. As shown in Fig. 2, while peak position stays at 8.4° for all EAA/ATT composites, the peak intensity increases with the increment of ATT loadings. Therefore, ATT maintains its unique structure even after the curing reaction in the EAA system. The broad peaks of EAA/ATT composites at about 20° show the noncrystalline state of EA materials, which also have not been changed by the addition of ATT. Similar results were also reported in poly(butylene succinate-co-butylene adipate)/ATT composites [17].

3.2. Rheological properties

Unlike other thermoplastic polymer modified asphalt, epoxy asphalt is one of the reactive polymer modified asphalts. Cure reaction will take place as long as the epoxy monomers and hardeners are mixing. The increment of molecular weight of epoxy will inevitably result in the increase of EAA's viscosity [18]. If the viscosity is too high, the EAA layer will be hard to be paved on the surface of steel bridge decks or concretes. Therefore, the viscosity of EAA needs to be well controlled. Fig. 3 shows the rotational viscosity-time curves of the neat EAA and EAA/ATT composites at 120 °C. The rotational viscosities of EAA/ATT composites are all lower than that of the neat EAA at a specific cure time. Furthermore, the higher ATT loading is, the longer time required to reach the same viscosity. Viscosity decline coming along with the ATT loading increase may stem from the hindrance effect of fibrous nanoclays on the molecular movement of epoxy monomers, hardeners and asphalts [19]. According to the general specifications of epoxy asphalt materials for paving roads and bridges, the viscosity of EAA to 1000 mPa s at 120 °C needs to be over 10 min [20]. As shown in Fig. 3, the time of the neat EAA and EAA with 1, 3 and 5 wt% ATT to reach 1000 mPa s at 120 °C is 14, 24, 25 and 35 min, respectively. The hindrance effect of fibrous nanoclays prolongs the construction time of EAA. However, it is worth to note that the viscosity will affect the thickness of adhesive bond line. If the viscosity is too low, the flowability of the adhesive would increase and result in a thin bond line. Eventually, this will weaken the adherence of the adhesive.

3.3. Thermal stability

During the construction of steel bridge deck, hot bituminous mixtures will be paved on the surface of the EAA layer. Therefore, EAA is needed to have excellent thermal stability to resist the thermal shock from the hot bituminous mixtures. The TGA and derivative thermogravimetric (DTG) curves of the neat ATT, the neat EAA and EAA/ATT composites are shown in Fig. 4. As depicted in Fig. 4, the thermal degradation of ATT can be divided into three stages. The first stage at around 100 °C relates to the loss of surface absorption water. The second stage at 100–200 °C corresponds to the removal of crystal water and zeolitic water. The last stage at 300–500 °C ascribes to the loss of hydroxyl groups [21]. Unlike the neat ATT, TGA curves of both the neat EAA and EAA/ATT composites present one-stage thermal degradation, indicating the addition of ATT does not change the degradation process of the neat EAA.

Table 1 lists the initial decomposition temperature (IDT, the temperature at 10% weight loss), the integral procedural decomposition temperature (IPDT), temperature at the maximum degradation rate (T_{max}) and char residues at 600 °C of the neat ATT, the neat EAA and ATT/EAA composites. As shown in Table 1, the IDTs of EAA/ATT composites are slightly higher than that of the neat EAA (299.0 °C). The

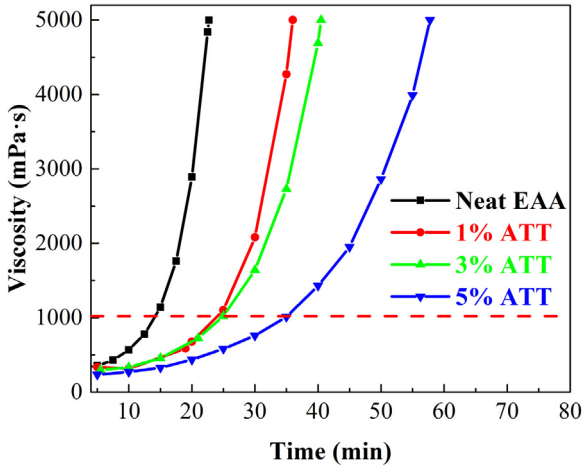

Fig. 3. Viscosity-time curves of the neat EAA and EAA/ATT composites at 120 °C.

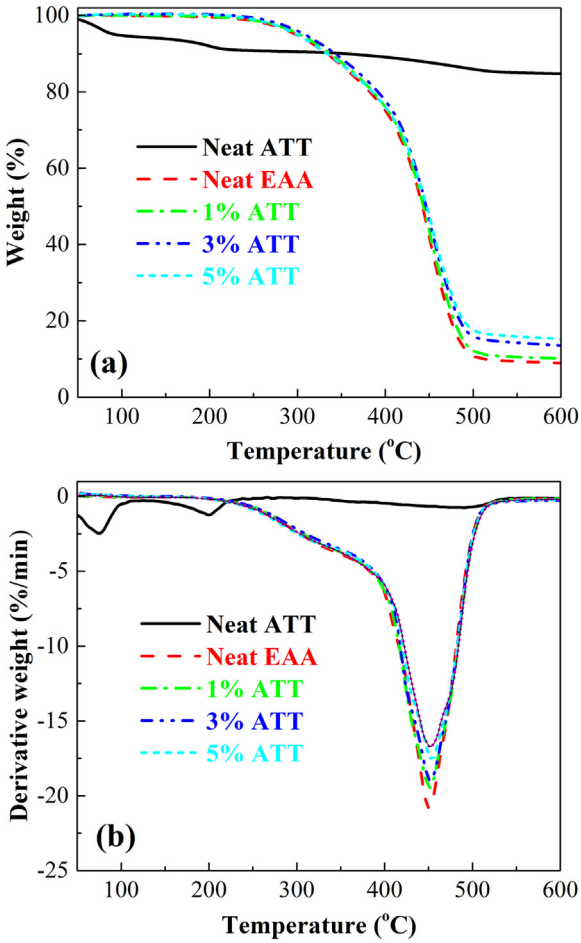

Fig. 4. TGA (a) and DTG (b) curves of the neat ATT and EAA/ATT composites.

Table 1
TGA and DTG results of ATT, neat EAA and EAA/ATT composites.

ATT (wt%)	IDT (°C)	IPDT (°C)	T_{max} (°C)	Residue at 600 °C (%)
100	93.4	–	75.2, 198.7, 491.0	64.3
0	299.0	492.0	450.3	8.9
1	303.2	504.5	450.8	10.1
3	308.7	539.3	452.1	13.5
5	299.9	554.6	454.1	15.3

composite with 3 wt% ATT has the highest IDT (308.7 °C). The IPDT of samples increases from 492.0 to 554.6 °C when the ATT loading increases from 0 wt% to 5 wt%. The T_{max} of EAA/ATT composites is slightly higher than that of the neat EAA. These results indicate that the addition of ATT enhances the thermal stability of the neat EAA. Particular barrier effect of the nanoclay could slow down the thermal transportation of the polymer matrix, leading to the enhancement of the thermal stability. However, metal ions carried by ATT are able to increase the decomposition rate of the polymer [22]. Dominance of barrier effect in the case of low ATT loading may explain the improvement of thermal stability of EAA/ATT composites. Nevertheless, metal ions-driven degradation effect becomes dominant in the composite containing highest ATT loading (5 wt%). Thus, the IDT of EAA composite with 5 wt% ATT slightly reduces compared to that of EAA composite with 3 wt% ATT. The char residues at 600 °C of EAA/ATT composites increase with the increase of ATT loadings. This is because char residues from the neat ATT is well above residues from all other composites (Table 1). Similar results were also found in nylon 6/ATT composites [23]. Therefore, it can be concluded that the incorporation of ATT improves the thermal stability of the EAA layer to resist the thermal shock of the hot bituminous mixtures.

3.4. Mechanical properties

Fig. 5 illustrates the stress-strain curves of the neat EAA and EAA/ATT composites. The neat EAA exhibits a ductile deformation with the appearance of a lower yield point, which is in accord with EA binders [24]. The addition of ATT increases the stiffness of the neat EAA. Tensile strength, elongation at break, toughness and Young's modulus are summarized in Table 2. The addition of ATT increases both tensile strength and Young's modulus of the neat EAA. Besides, both tensile strength and Young's modulus increase with the increase of ATT loadings. Similar results were also reported in polyurethane (PU)/ATT composites [25–27]. In addition, this increment tendency was even kept to 12 wt% ATT loading. However, the viscosity needs to be well controlled in the construction of the neat EAA. As discussed above, higher ATT loading results in the lower viscosity of EAA and thin bond line during construction. Thus, the effect of higher loadings on the mechanical properties of the neat EAA is not considered in this paper. The EAA composite with 5 wt% ATT has the maximum tensile strength (8.72 MPa) and Young's modulus (90.62 MPa), which are 56% and 40% greater than those of the neat EAA (5.59 MPa and 64.81 MPa), respectively. It is well accepted that the tensile strength of polymeric material depends on the cohesive energy of the material. The tensile strength increase in the presence of ATT is directly attributed to the reinforcement provided by the well dispersed ATT particles and strong

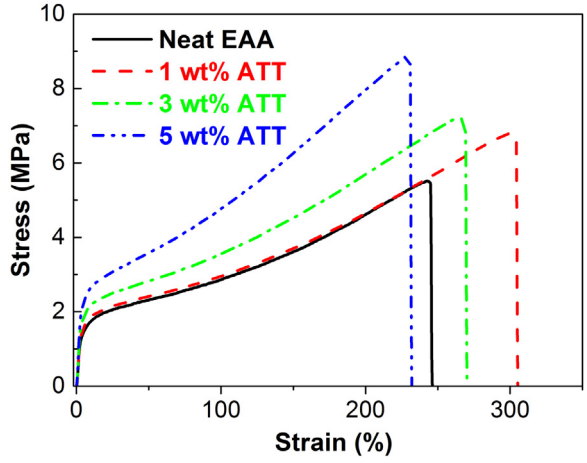

Fig. 5. Stress-strain curves of the neat EAA and EAA/ATT composites.

Table 2
Mechanical properties of the neat EAA and EAA/ATT composites.

ATT (wt %)	Tensile strength (MPa)	Elongation at break (%)	Toughness (MPa)	Young's modulus (MPa)
0	5.59 ± 0.58	237 ± 11	835.3 ± 127.1	64.81 ± 13.32
1	7.01 ± 0.68	311 ± 28	1124.9 ± 85.2	67.80 ± 6.37
3	7.05 ± 0.23	259 ± 32	1174.4 ± 76.3	78.40 ± 4.20
5	8.72 ± 0.68	220 ± 10	1269.7 ± 50.6	90.62 ± 16.71

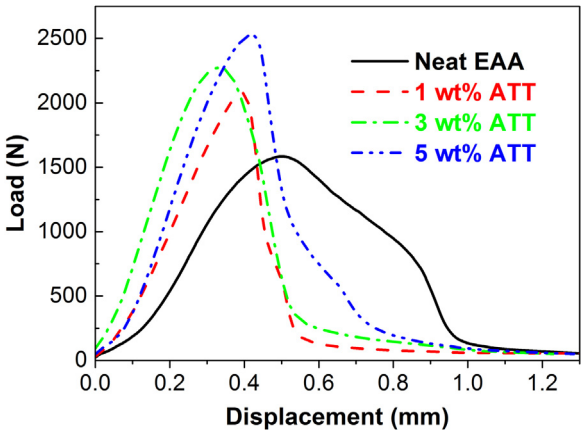

Fig. 6. Load-displacement curves of the neat EAA and EAA/ATT composites.

Table 3
Adhesive properties of the neat EAA and EAA/ATT composites.

ATT (wt%)	Adhesive strength (MPa)
0	6.05 ± 0.80
1	6.67 ± 0.89
3	7.49 ± 1.37
5	7.58 ± 0.59

interfacial interactions between ATT and the EAA matrix.

The addition of ATT increases the elongation at break of the neat EAA in the case of loading lower than 3 wt%. For EAA composites, the elongation at break reaches the maximum value at the ATT loading of 1 wt%, which is 31% higher than that of the neat EAA. With the increase of ATT loadings, the elongation at break slightly decreases and this percentage of EAA composite with 5 wt% ATT is slightly lower than that of the neat EAA. It is worth to mention that all the tensile strength and elongation at break of EAA/ATT composites meet the general specifications of epoxy asphalt materials for paving roads and bridges, whose values are 6.0 MPa and 190%, respectively [20]. It is known that the area under stress-strain curve represents the total work per unit volume consumed by the material for fracture. In general, the improvement of tensile strength is always accompanied by a sacrifice in the toughness. As shown in Table 2, however, the addition of ATT enhances the toughness of the neat EAA. Moreover, the toughness of EAA/ATT composites increases with the increase of ATT loadings. The toughness of the EAA composite with 5 wt% ATT (1269.7 MPa) is 52% greater than that of the neat EAA (835.3 MPa).

3.5. Adhesive strength

The load versus displacement curves of the neat EAA and EAA/ATT composites resulting from the shear lap tests are shown in Fig. 6. It can be seen that the load increases nonlinearly with the increasing displacement and then drops gradually at failure due to high toughness of the neat EAA and its ATT composites as discussed above. The figure also

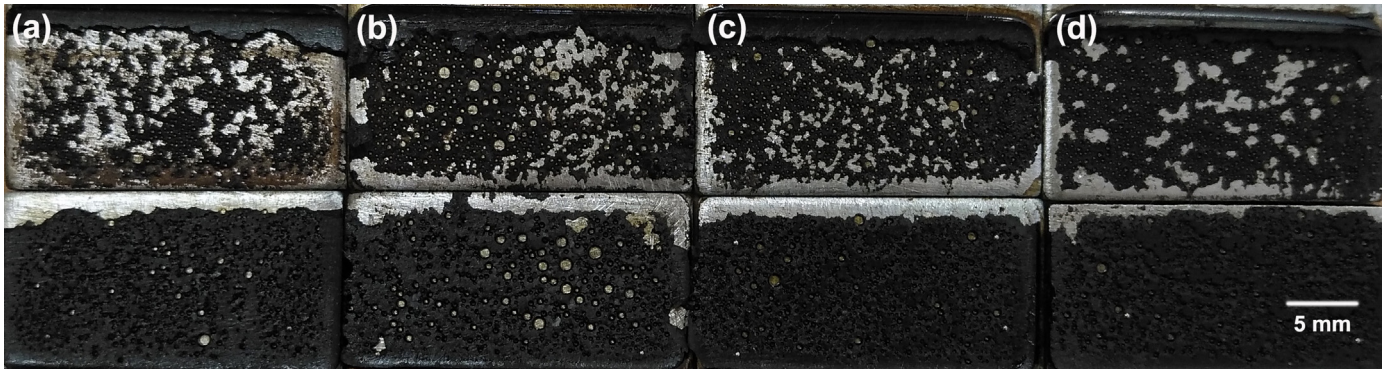

Fig. 7. Failure profiles of bonded steel plates after single-lap shear tests: (a) neat EA, (b) 1 wt% ATT, (c) 3 wt% ATT and (d) 5 wt% ATT.

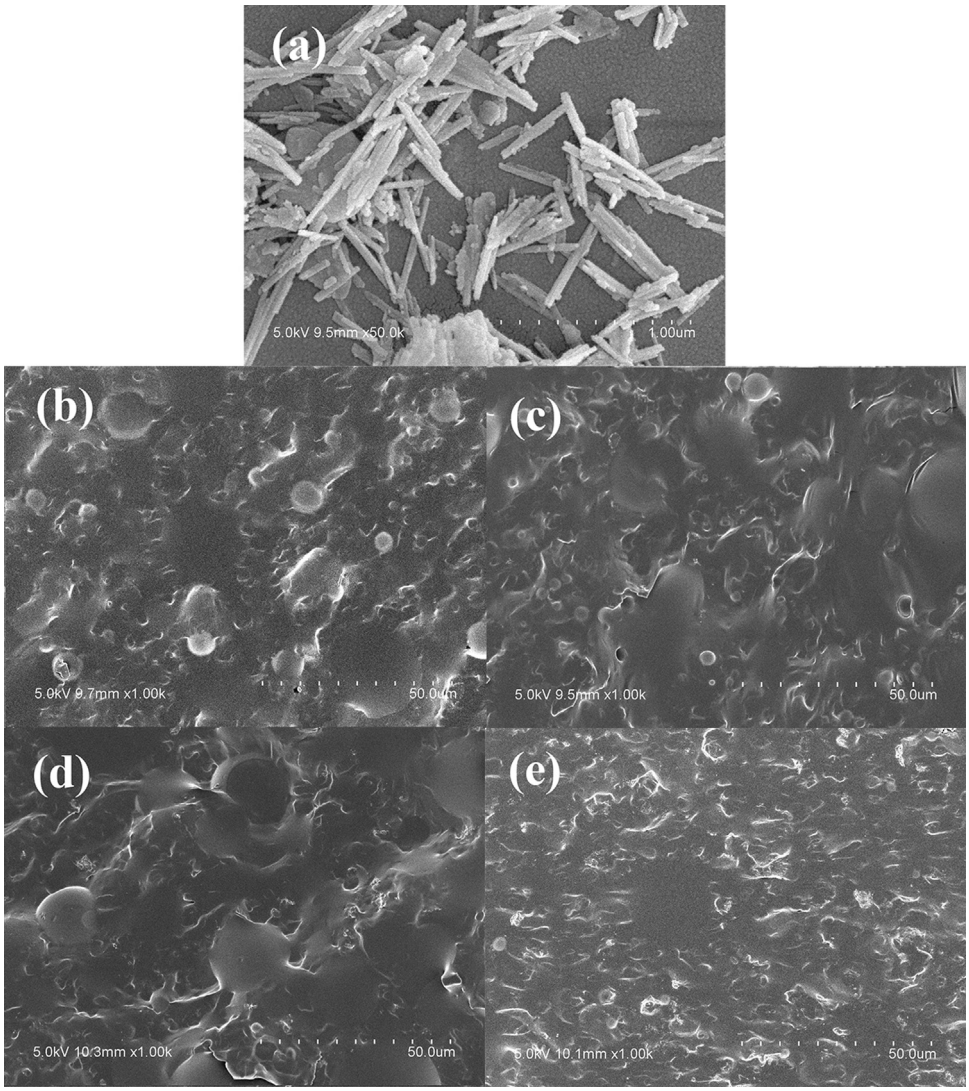

Fig. 8. SEM micrographs of the neat ATT (a), the neat EAA (b) and EAA/ATT composites with different ATT contents: 1 wt% (c), 3 wt% (d) and 5 wt% (e).

reveals that there exists strengthening of shear resistance as a result of dispersed ATT particles, as evidenced by the increase in the critical shear loads with the critical load.

From the load displacement curve, adhesive strength was estimated using the Eq. (1) and summarized in Table 3. Obviously, the addition of ATT increases the adhesive strength of the neat EAA. Furthermore, the adhesive strength of EAA/ATT composites increases with the increase of fibrous nanoclay loadings. The adhesive strength of the EAA composite with 5 wt% ATT achieves the highest value (7.58 MPa), which elevates by 25% compared to that of the neat EAA (6.05 MPa). Fig. 7 presents failure profiles of bonded steel plates after single-lap shear tests. It can be observed that the adhesive failure takes place predominately between EAA layers. In addition, due to the reinforced effect of ATT, the areas of the rest of EAA on the steel plates increase with the increase ATT contents, which agree well with the monotonously incremental tendency of the adhesive strengths. These results

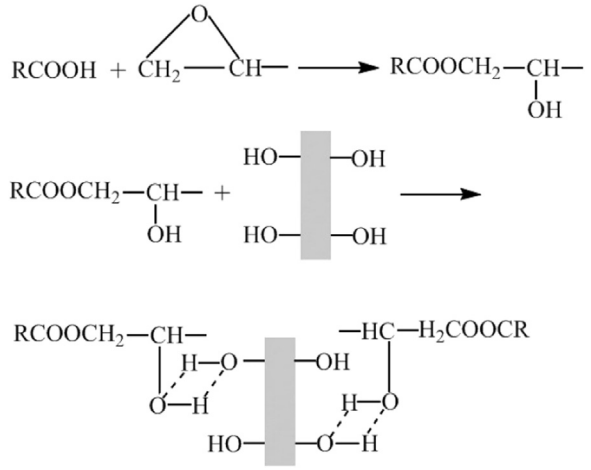

Fig. 9. Schematic representation of reaction between hydroxyl groups of epoxy and hydroxyl groups on the surface of ATT.

indicate that the adhesive strength of EAA/ATT composites probably relates to the dispersion of the fibrous nanoclay in the polymer matrix and the increase of the Young's modulus presented on the Table 2. In other words, the adhesive strength is probably not linked to the adhesion of the composite to the steel plate, but relates to the composite cohesion only.

3.6. Morphology

SEM micrographs for the neat EAA and EAA/ATT composites are shown in Fig. 8. Fig. 8a presents fibrous ATT crystals with diameters of about 20–70 nm and lengths of less than 1 μm. As shown in Fig. 8b-e, two distinct phases appear in the neat EAA and its ATT composites, where epoxy resin is the continuous phase and asphalt is the disperse phase. Similar morphology was also observed by other researchers [28]. Evidently, the addition of ATT does not change the phase separation of EAA. Due to the existence of phase separation, the dispersion of ATT in the EAA matrix is hard to be observed. Therefore, it is difficult to relate the aforementioned enhancement of tensile and bonding properties to the dispersion of ATT in the epoxy matrix. As discussed above, XRD results indicate that the structure of ATT is not altered during the cure reaction of the neat EAA. Unlike montmorillonite, therefore, the increment of tensile strength and modulus of the neat EAA does not benefit from clay exfoliation in the epoxy matrix.

Fig. 9 shows schematic representation of reaction between hydroxyl groups of epoxy and hydroxyl groups on the surface of ATTs. It is known that hydroxyl groups will be released when epoxide groups of epoxy monomers react with curing agents. In addition, the formed hydroxyl groups in the EAA matrix will continue to interact with the abundant hydroxyl groups on the surface of ATTs via hydrogen bonding [29], resulting in the increment of aforementioned mechanical properties the neat EAA. In addition, the adherence of the nanofiller reinforced adhesive depends not only on the interfacial interaction between the adhesive and the substrate but also on the interfacial interaction between the nanofiller and the polymer matrix. Thus, the increment of mechanical properties with the addition of ATT also facilitates the enhancement of adhesive strength of the neat EAA.

4. Conclusion

In this paper, epoxy asphalt adhesive/attapulgite composites were prepared and characterized. The existence of ATT has little effect on the noncrystalline structure of the neat EAA. The addition of ATT lowers the rotational viscosity of the neat EAA during the cure reaction. The viscosity of EAA/ATT composites decreases with the increase of ATT loadings at a specific curing time. The presence of ATT improves the thermal stability of the neat EAA and increases the ability of the EAA layer to resist the thermal shock of the hot bituminous mixtures. Moreover, with the increase of ATT loading, the tensile strength, toughness, Young's modulus of EAA/ATT composites increase. Compared to the neat EAA, the addition of 5 wt% ATT increases the tensile strength, toughness and Young's modulus of the EAA composite by 56%, 52% and 40%, respectively. Except for 5 wt% loading, the inclusion of ATT enhances the elongation at break of the neat EAA. The elongation at break of the neat EAA increases 31% with adding 1 wt% ATT. Meanwhile, the presence of ATT increases the adhesive strength of the neat EAA. The adhesive strength of EAA/ATT composites increases with the increase of ATT loadings. The addition of fibrous nanoclay increases the adhesive strength of the neat EAA by 25% with 5 wt% ATT.

Acknowledgements

The authors are grateful for financial supports from Program for Changjiang Scholars and Innovative Research Team in University (IRT1252), the Priority Academic Program Development of Jiangsu Higher Education Institutions, and the Fundamental Research Funds for the Central Universities (20620140066). Dr. Weijing Liu and Dr. Xiaoshan Wang are greatly appreciated for manuscript preparation.

Conflicts of interest

None.

References

[1] Liu Y, Zhang J, Chen R, Cai J, Xi Z, Xie H. Ethylene vinyl acetate copolymer modified epoxy asphalt binders: phase separation evolution and mechanical properties. Constr Build Mater 2017;137:55–65.
[2] Liu Y, Zhang J, Jiang Y, Li C, Xi Z, Cai J, et al. Investigation of secondary phase separation and mechanical properties of epoxy SBS-modified asphalts. Constr Build Mater 2018;165:163–72.
[3] Zhang Y, Pan X, Sun Y, Xu W, Pan Y, Xie H, et al. Flame retardancy, thermal, and mechanical properties of mixed flame retardant modified epoxy asphalt binders. Constr Build Mater 2014;68:62–7.
[4] Kang Y, Wu Q, Jin R, Yu PF, Cheng JQ. Rubber-like quasi-thermosetting polyetheramine-cured epoxy asphalt composites capable of being opened to traffic immediately. Sci Rep 2016;6:18882.
[5] Lu Q, Bors J. Alternate uses of epoxy asphalt on bridge decks and roadways. Constr Build Mater 2015;78:18–25.
[6] Jia X, Huang B, Chen S, Shi D. Comparative investigation into field performance of steel bridge deck asphalt overlay systems. KSCE J Civil Eng 2016;20:2755–64.
[7] Yao B, Li FC, Wang X, Cheng G. Evaluation of the shear characteristics of steel-asphalt interface by a direct shear test method. Int J Adhes Adhes 2016;68:70–9.
[8] Bradley W. The structural scheme of attapulgite. Am Miner 1940;25:405–10.
[9] Ruiz-Hitzky E, Darder M, Alcantara ACS, Wicklein B, Aranda P. Recent advances on fibrous clay-based nanocomposites. In: Kalia S, Haldorai Y, editors. Organic-inorganic hybrid nanomaterials. Cham: Springer Int Publishing Ag; 2015. p. 39–86.
[10] Lu H, Shen H, Song Z, Shing KS, Tao W, Nutt S. Rod-like silicate-epoxy nanocomposites. Macromol Rapid Commun 2005;26:1445–50.
[11] Xue S, Reinholdt M, Pinnavaia TJ. Palygorskite as an epoxy polymer reinforcement agent. Polymer 2006;47:3344–50.
[12] Zhao L, Zhan G, Yu Y, Tang X, Li S. Influence of attapulgites on cure-reaction-induced phase separation in epoxy/poly(ether sulfone) blends. J Appl Polym Sci 2008;108:953–9.
[13] Niu X, Huo L, Cai C, Guo J, Zhou H. Rod-like attapulgite modified by bifunctional acrylic resin as reinforcement for epoxy composites. Ind Eng Chem Res 2014;53:16359–65.
[14] Zhang J, Wang J, Wu Y, Sun W, Wang Y. Investigation on thermo-rheological properties and stability of SBR modified asphalts containing palygorskite clay. J Appl Polym Sci 2009;113:2524–35.
[15] Sun Y, Zhang Y, Xu K, Xu W, Yu D, Zhu L, et al. Thermal, mechanical properties, and low-temperature performance of fibrous nanoclay-reinforced epoxy asphalt composites and their concretes. J Appl Polym Sci 2015;132:41694.
[16] Chisholm JE. An X-ray powder-diffraction study of palygorskite. Can Miner 1990;28:329–39.
[17] Qi ZG, Ye HM, Xu J, Chen JN, Guo BH. Improved the thermal and mechanical properties of poly(butylene succinate-co-butylene adipate) by forming nanocomposites with attapulgite. Colloids Surf A: Physicochem Eng Asp 2013;421:109–17.
[18] Liu Y, Xi Z, Cai J, Xie H. Laboratory investigation of the properties of epoxy asphalt

rubber (EAR). Mater Struct 2017;50:219.
[19] Esmizadeh E, Naderi G, Yousefi AA, Milone C. Investigation of curing kinetics of epoxy resin/novel nanoclay–carbon nanotube hybrids by non-isothermal differential scanning calorimetry. J Therm Anal Calorim 2016;126:771–84.
[20] GB/T 30598. General specifications of epoxy asphalt materials for paving roads and bridges. Beijing: Standards Press of China; 2014.
[21] Frost RL, Ding Z. Controlled rate thermal analysis and differential scanning calorimetry of sepiolites and palygorskites. Thermochim Acta 2003;397:119–28.
[22] Yuan XP, Li CC, Guan GH, Xiao YN, Zhang D. Thermal degradation investigation of poly (ethylene terephthalate)/fibrous silicate nanocomposites. Polym Degrad Stab 2008;93:466–75.
[23] Shen L, Lin YJ, Du QG, Zhong W. Studies on structure–property relationship of polyamide-6/attapulgite nanocomposites. Compos Sci Technol 2006;66:2242–8.
[24] Yin H, Jin H, Wang C, Sun Y, Yuan Z, Xie H, et al. Thermal, damping, and mechanical properties of thermosetting epoxy-modified asphalts. J Therm Anal Calorim 2014;115:1073–80.
[25] Wang C, Ding L, Wu Q, Liu F, Wei J, Lu R, et al. Soy polyol-based polyurethane modified by raw and silylated palygorskite. Ind Crop Prod 2014;57:29–34.
[26] Wang C, Wu Q, Liu F, An J, Lu R, Xie H, et al. Synthesis and characterization of soy polyol-based polyurethane nanocomposites reinforced with silylated palygorskite. Appl Clay Sci 2014;101:246–52.
[27] Wang C, Wang Y, Liu W, Yin H, Yuan Z, Wang Q, et al. Natural fibrous nanoclay reinforced soy polyol-based polyurethane. Mater Lett 2012;78:85–7.
[28] Yin H, Zhang Y, Sun Y, Xu W, Yu D, Xie H, et al. Performance of hot mix epoxy asphalt binder and its concrete. Mater Struct 2015;48:3825–35.
[29] Lei Z, Yang Q, Wu S, Song X. Reinforcement of polyurethane/epoxy interpenetrating network nanocomposites with an organically modified palygorskite. J Appl Polym Sci 2009;111:3150–62.